

## First results from a marine controlled-source electromagnetic survey to detect gas hydrates offshore Oregon

K. A. Weitemeyer, S. C. Constable, K. W. Key, and J. P. Behrens

Scripps Institution of Oceanography, University of California, San Diego, La Jolla, California, USA

Received 13 October 2005; revised 13 December 2005; accepted 19 December 2005; published 3 February 2006.

[1] Submarine gas hydrate is a hazard to drilling, a potential hydrocarbon resource, and has been implicated as a factor in both submarine slope stability and climate change. Bulk in situ electrical resistivities evaluated from electromagnetic surveys have the potential to provide an estimate of the total hydrate volume fraction more directly than by using seismic and well log data. We conducted a marine controlled-source electromagnetic sounding at Hydrate Ridge, Oregon, USA, in August, 2004. Electromagnetic fields transmitted by a deep-towed horizontal electric dipole source were measured by a linear array of 25 seafloor electromagnetic receivers, positioned 600 m apart to produce a dense coverage in the recorded electric field data. Results are presented in simple form by apparent resistivity pseudosections, which produce an approximate image of lateral resistivity variations across the study region. Resistivity values are consistent with those from well logs collected in the area and pseudosection features are correlated with seismic reflectors. Archie's Law, based on pseudosection apparent resistivities, predicts volumetric hydrate concentrations vary from 0–30% across the ridge. **Citation:** Weitemeyer, K. A., S. C. Constable, K. W. Key, and J. P. Behrens (2006), First results from a marine controlled-source electromagnetic survey to detect gas hydrates offshore Oregon, *Geophys. Res. Lett.*, *33*, L03304, doi:10.1029/2005GL024896.

### 1. Introduction

[2] Natural gas hydrates are a hazard to drilling, infrastructure, and slope stability; hydrates are also considered to play a significant role in global climate change and in the carbon cycle [Kvenvolden, 2000]. The large quantities of methane contained in hydrate found in marine and permafrost regions worldwide, estimated to be  $10^{16}$  kg, has generated interest in gas hydrates as a future energy resource [Buffett, 2000]. However, there is no reliable method for mapping and quantifying natural gas hydrates in situ. We explore the use of electromagnetic (EM) methods for this purpose.

[3] The common natural gas hydrate consists of a methane molecule encased by a water lattice. High pressures and cool temperatures are required for hydrate stability; at ocean depths greater than 300 m and temperatures around 0°C, methane concentrations in excess of solubility will cause the formation of methane hydrate [Kvenvolden, 2003]. Perturbations in pressure or temperature can cause the rapid release of methane from hydrate.

[4] Seismic methods are often used to detect hydrates; a bottom simulating reflector (BSR) sometimes marks the phase boundary of solid hydrate above and free gas below the BSR [Shipley *et al.*, 1979]. The BSR depth is controlled by the intersection of the hydrate stability field with the local geothermal gradient. While seismic methods are often able to detect the lower stratigraphic bound of hydrate, the diffuse upper bound is not well imaged and there is no seismic reflectivity signature from within the hydrate region. Finally, there are cases where hydrates are known to exist, yet exhibit no BSR [Sloan, 1990].

[5] Other methods for hydrate detection include electrical resistivity measurements both from well logs and from controlled-source electromagnetic (CSEM) methods. Electrical resistivity logs indicate an increase in resistivity from zones containing hydrate when compared with water saturated zones [e.g., Collett and Ladd, 2000]. Although this effect can be modest, it provides a suitable EM target for the detection of hydrates. The EM response increases with an increase in hydrate volume fraction.

[6] The CSEM technique has been developed primarily from academic research [e.g., Chave *et al.*, 1991]. The application for hydrate detection was first considered by Edwards [1997]; he modeled the transient electric dipole-dipole method as a means of estimating hydrate volume and argued for the usefulness of EM methods in augmenting seismic and drilling techniques. Field studies conducted at the Cascadia margin off the west coast of British Columbia [Yuan and Edwards, 2000; Schwalenberg *et al.*, 2005] have demonstrated the merits of this technique by revealing the presence of hydrates when no BSR or other seismic signature exists.

[7] A pilot marine EM study at Hydrate Ridge, Oregon, was conducted in August 2004. The CSEM method we employed is a frequency domain technique described by Chave and Cox [1982] and Constable and Cox [1996], and has recently been extended to hydrocarbon exploration [e.g., Eidesmo *et al.*, 2002]. A horizontal electric dipole source is towed on or close to the seafloor and receivers anchored on the seafloor record the transmitted fields at various ranges and frequencies. Extensive CSEM and magnetotelluric data were acquired for our study; here we present first results from one CSEM transect.

### 2. Hydrate Ridge

[8] Located 80 km off-shore from Newport, Oregon, Hydrate Ridge is situated on an accretionary ridge, part of the Cascadia subduction zone, and is in water depths of 820–1200 m (Figure 1). Hydrate Ridge has been extensively studied using seismic methods, by the Ocean Drilling

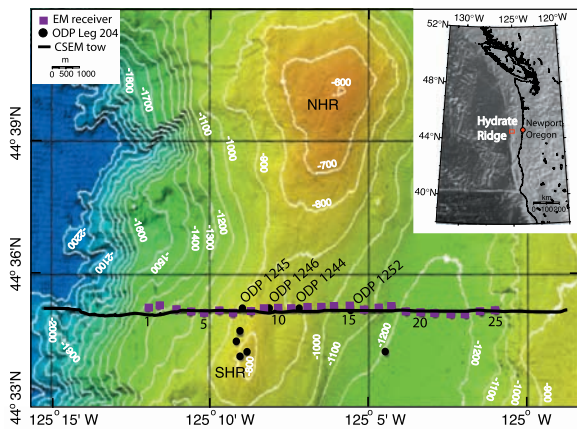


**Figure 1.** Bathymetric map of survey area at southern Hydrate Ridge (SHR) (from MBARI multibeam survey, 2001). Inset shows regional location (ETOPO2 global relief from NOAA, 2001). NHR, northern Hydrate Ridge.

Program (ODP), with remotely operated vehicles, and by acoustic bathymetry mapping [Tréhu and Bangs, 2001; Shipboard Scientific Party, 2003; Clague et al., 2001]. These data sets allow a comprehensive comparison with our CSEM results.

[9] Considerable concentrations of gas hydrate, derived from thermogenic and microbial decomposition of organic matter, exist at Hydrate Ridge [Torres et al., 2004]. The distribution is inferred from the BSR, which covers much of the 25 km by 15 km area [Shipboard Scientific Party, 2002] at a depth of about 130 meters below seafloor (mbsf). ODP Leg 204 well logs place further constraints on the distribution and concentration of hydrates. Generally, hydrates occur in lenses in a region from 45 mbsf to the BSR, however at the summit of southern Hydrate Ridge (SHR) massive gas hydrate outcrops [Shipboard Scientific Party, 2003, 2002]. Along the northern flank of SHR the concentrations vary from 1% to 8% based on correlation of different hydrate proxies from well logs [Tréhu et al., 2004].

### 3. Experimental Methods and Data Analysis

[10] Forward modeling studies using a 1-D layered code [Flosadóttir and Constable, 1996] reveal that the hydrate anomaly should exhibit the largest signal in radial mode (when source and receiver dipoles are in line) electric fields at high frequencies ( $>10$  Hz). Fields at these high frequencies attenuate very quickly. To create a wide window of detectable ranges (200–2500 m) associated with the hydrate anomaly we transmitted a lower frequency square wave at 5 Hz and processed both the fundamental (5 Hz) and the first odd harmonic (15 Hz).

[11] Twenty-five seafloor EM receivers [Constable et al., 1998] were placed in a linear west-east array at a 600 m instrument spacing across the northern flank of SHR (Figure 1). This array coincides with four ODP well logs (1244, 1245, 1246, 1252) and seismic line 230 [Tréhu and Bangs, 2001], which sample the ridge and the slope basin to the east. The CSEM transmissions were done using a 90 m antenna with dipole moment 1.15 kA-m. The transmitter was towed 100 m above the seafloor for 10 hours, equivalent to a

20 km line of data. Locations of receivers and transmitter were obtained using long baseline acoustic navigation.

[12] Electric field time series from the receivers are Fourier transformed to the frequency domain within stack frames of 2 minutes and the results are merged with the navigated source–receiver offset. We calculate the major axis of the electromagnetic polarization ellipse (Pmax) for the horizontal electric fields because it is insensitive to receiver orientation and is less sensitive to transmitter orientation [Constable and Cox, 1996]. Figure 2 shows Pmax versus source–receiver offset for the receiver at site 5 (s5). The 5 Hz data are above the instrumental noise floor to a 2.5 km range and the 15 Hz data to a range of 1.5 km. The 5 Hz electric fields are stronger when the transmitter is 2 km west of the receiver, indicative of a resistive feature in the subsurface.

[13] We convert the 5 Hz and 15 Hz electric field data at each receiver and each range into equivalent half-space resistivity using the 1-D layered code [Flosadóttir and Constable, 1996] and obtain values between 1 and 3  $\Omega$ -m, which are similar to the four ODP well logs (Figure 3e). To gain an understanding of the subsurface structure without involving the complication of a 2-D inversion we map resistivities to depths in a similar manner to the DC resistivity pseudosection, in essence creating a CSEM apparent resistivity pseudosection. We assume that the resistivities at each range can be mapped into an equivalent depth by means of a common midpoint between the receiver and the transmitter projected at a 45 degree angle from the seabed. This method, while limited, does provide insight into the lateral heterogeneity in the data. However, unlike DC resistivity the depth is not purely geometric.

### 4. Results

[14] Reciprocity between transmitter and receiver creates a two fold redundancy in the pseudosection from east-side and west-side transmission data. The east-side and west-side transmission data sets are compatible, so we averaged them using a regularized contouring algorithm to obtain a 2-D map of apparent resistivity. The 15 Hz and 5 Hz pseudosections are shown in Figures 3a and 3b. The 15 Hz data are sensitive to shallower sediment than the 5 Hz data. This is reflected by a general agreement of the 15 Hz pseudosection with the shallow part of the 5 Hz pseudosection.

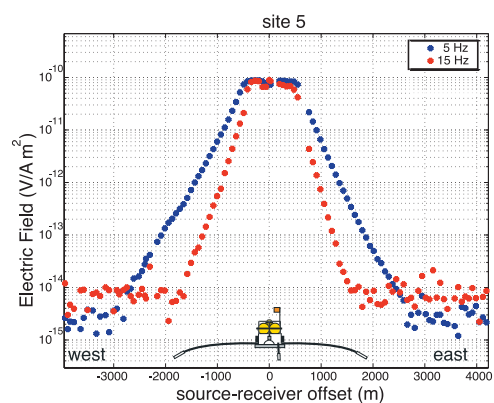


**Figure 2.** Major axis of the electromagnetic polarization ellipse (Pmax) versus range for site 5 at 5 Hz and 15 Hz.

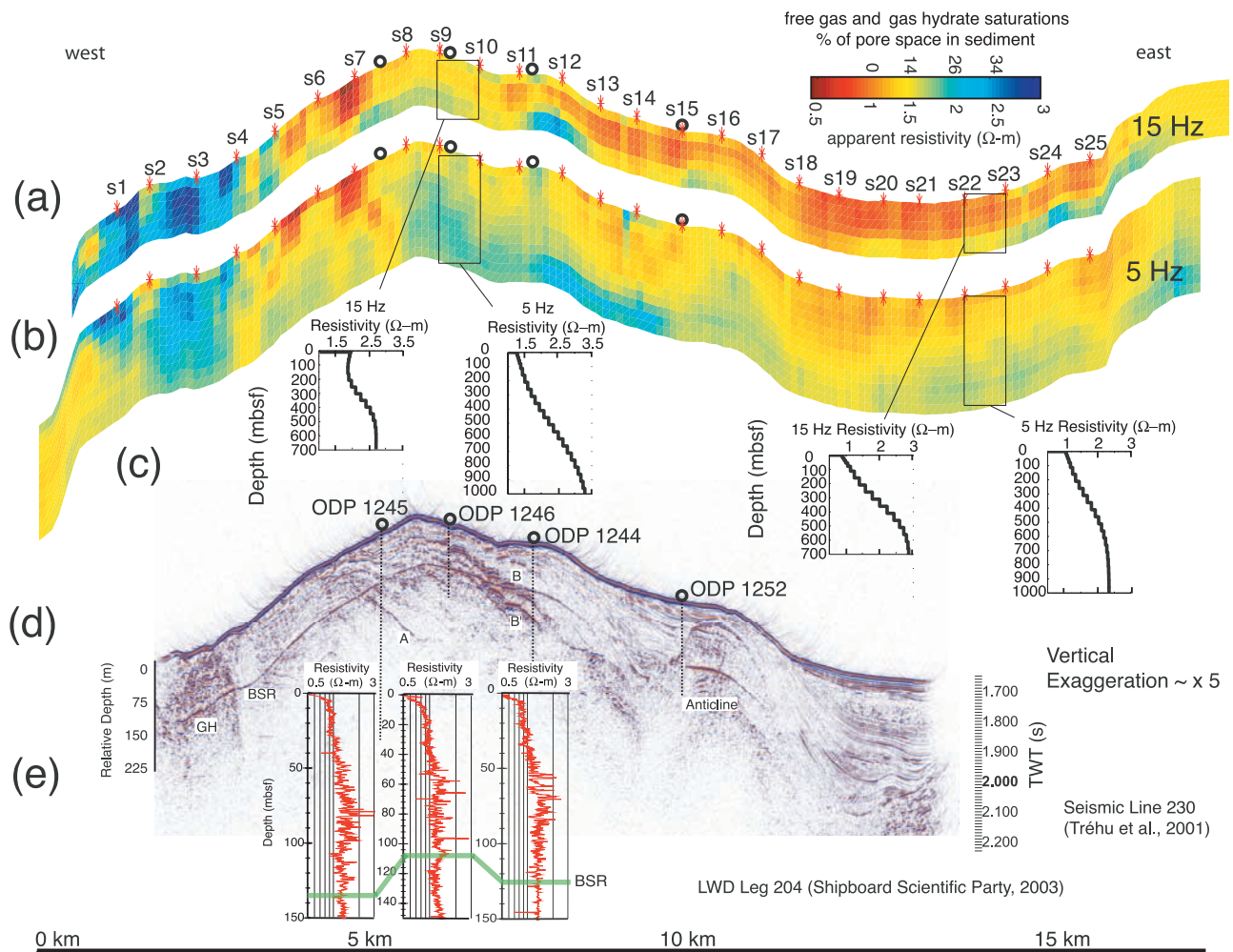


**Figure 3.** Pseudosection results for (a) 15 and (b) 5 Hz data, with a combined apparent resistivity and gas hydrate saturation scale; (c) 1-D inversions for marked locations; (d) seismic line 230, and (e) logging-while-drilling (LWD) deep resistivity logs. GH, gas hydrate or free gas inferred from a seismic inversion [Zhang and McMechan, 2003]; BSR, bottom simulating reflector; A, B, B', seismic horizons explained in text. ODP Leg 204 sites are marked on seismic section. EM receiver sites are marked by red asterisk.

[15] The pseudosections exhibit significant lateral variations in resistivity. The basin to the east (s18–s25) is more conductive than the ridge (s4–s17), consistent with estimates of higher concentrations of hydrates at the ridge and lesser concentrations of hydrate in the basin [Tréhu et al., 2004]. Below s16 and s17 there is a resistive feature in the 5 Hz data associated with the anticline and possibly reflecting a change in lithologic composition. This feature is barely seen in the 15 Hz data which suggests that it is deeper. The high resistivity seen in the 5 Hz data below s8–s15 could be associated with seismic horizons B and B', which consist of highly resistive layers as indicated in the logging while drilling data at ODP 1246 (Figure 3e) [Shipboard Scientific Party, 2003]. The largest CSEM resistivities are along the western end of the profile (GH in Figure 3d), consistent with the inference of high hydrate and free gas saturations from seismic velocity inversions [Zhang and McMechan, 2003].

[16] The conductive feature projecting from s6 is anomalous. It could be that the electric field sensors are sitting directly over a conductor, such as a brine, and the pseudosection projection method is causing the pant-leg appear-

ance. This is not unreasonable considering that brines exist to the south at ODP 1249 and 1250 [Torres et al., 2004]. On the other hand, horizon A (Figure 3) is known to be a highly porous layer lined in ash that acts as a fluid conduit for methane gas to migrate to the summit of SHR [Shipboard Scientific Party, 2003; Tréhu et al., 2004], and is marked by low resistivity in the well logs (ODP 1245, 1247, 1250, 1248) [Shipboard Scientific Party, 2003]. It is possible that s6 is recording low resistivity values associated with the high porosity of horizon A.

[17] To convert apparent resistivities into an approximate hydrate concentration we follow Collett and Ladd [2000] and ODP Leg 204 Initial Reports [Tréhu et al., 2003] for the calculation of hydrate saturations using the Archie equation:  $S_w = (a R_w / \phi^m R_t)^{1/n}$ . Here  $S_w$  is water saturation;  $R_w$  is resistivity of the formation water (equivalent to seawater = 0.33 Ω-m);  $R_t$  is formation resistivity taken from the CSEM pseudosection;  $\phi$  is porosity of the sediments taken as the average value of 65% for the gas hydrate stability zone [Tréhu et al., 2003, 2004]. The constants  $a$ ,  $m$  and  $n$  are empirical parameters in Archie's equation and are given as

$a = 1$ ,  $m = 2.8$ ,  $n = 1.9$  [Tréhu *et al.*, 2003]. A hydrate saturation is calculated using  $S_h = 1 - S_w$ . The resulting concentration (Figure 3a) ranges from 0–30%. Our calculations indicate the eastern basin has 0% hydrate concentration at the surface and increased concentration at depth, consistent with reported higher concentrations of hydrates just above the BSR [Shipboard Scientific Party, 2003]. On the ridge we obtain concentrations of 10%–15%, similar to 8% previously estimated [Tréhu *et al.*, 2004]. West of the ridge we obtain concentrations of 30%, a high value which could be the result of a mixture of hydrate and free gas. In general, hydrate concentrations calculated from pseudosections show consistency with those calculated from ODP well logs of 0–30% [Tréhu *et al.*, 2003]. However, EM derived concentrations are subject to any inaccuracies in Archie's equation and to our assumption of uniform values of  $\phi$ ,  $m$ ,  $n$ ,  $a$ , and  $R_w$  for the region.

[18] The basin structure appears to be one dimensional, so smooth 1-D inversions [Flosadóttir and Constable, 1996] of the data between s22 and s23 were carried out (Figure 3c). The transition from 1 to 2  $\Omega$ -m occurs at about 300 m depth in the 15 Hz inversion, and about 500 m in the 5 Hz inversion, providing some control on the depths of the corresponding features in the pseudosection projections. Similar inversions between s9 and s10 near ODP 1246 indicate higher resistivities at the ridge, but are probably not reliable for depth control because this region appears less 1-D in the pseudosections.

## 5. Conclusions

[19] Analysis of a new, comprehensive data set demonstrates the utility of the CSEM method for hydrate mapping. CSEM provides a more direct measure of bulk hydrate concentration than is possible with seismic reflectivity. The method estimates concentration in situ, in contrast to drilling, where sediments are altered and disturbed. The pseudosection approach developed for DC resistivity is a useful way to display lateral changes in resistivity for a linear and tightly spaced group of seafloor EM receivers. The bulk assessment of in situ hydrate resistivity provides a macroscopic measure of hydrate distribution for the region rather than a microscopic or point measurement given by well logs. These results are limited by uncertainty of Archie's Law as a conductivity-concentration relationship, and by the pseudosection imaging technique employed. Future work will involve obtaining resistivity and depth values from 2-D inversion and progress in laboratory measurements to characterize the electrical conductivity  $\sigma(\phi)$  relationship for seafloor hydrates.

[20] **Acknowledgments.** General funding for HyREX'04 was provided by the SIO Seafloor Electromagnetic Methods Consortium. Funds for ship time were provided by ExxonMobil and GERD, Japan. Thanks are extended to the Captain and Crew of the R.V. New Horizon and the technicians and engineers of the SIO Marine EM Laboratory. Thanks to Yamane Kazunobu, Adam Schultz, and Chester Weiss for assistance on the cruise. We particularly thank Ann Tréhu of Oregon State University for useful discussions prior to the experiment and for providing seismic line 230.

## References

Buffett, B. A. (2000), Clathrate hydrates, *Annu. Rev. Earth Planet. Sci.*, 28, 477–507.

- Chave, A. D., and C. Cox (1982), Controlled electromagnetic sources for measuring electrical-conductivity beneath the oceans: 1. Forward problem and model study, *J. Geophys. Res.*, 87, 5327–5338.
- Chave, A. D., S. C. Constable, and R. N. Edwards (1991), Electrical exploration methods for the seafloor, in *Electromagnetic Methods in Applied Geophysics*, edited by M. Nabighian, chap. 12, pp. 931–966, Soc. of Explor. Geophys., Tulsa, Okla.
- Clague, D. A., N. Maher, and C. K. Paull (2001), High-resolution multi-beam survey of Hydrate Ridge, offshore Oregon, in *Natural Gas Hydrates Occurrence, Distribution and Detection*, *Geophys. Monogr. Ser.*, vol. 124, edited by C. K. Paull and W. P. Dillon, pp. 297–304, AGU, Washington, D. C.
- Collett, T. S., and J. Ladd (2000), Detection of gas hydrate with downhole logs and assessment of gas hydrate concentrations (saturations) and gas volumes on the Blake Ridge with electrical resistivity log data, *Proc. Ocean Drill. Program Sci. Results*, 164, 179–191.
- Constable, S., and C. S. Cox (1996), Marine controlled-source electromagnetic sounding: 2. The PEGASUS experiment, *J. Geophys. Res.*, 101, 5519–5530.
- Constable, S., A. Orange, G. Hoversten, and H. F. Morrison (1998), Marine magnetotellurics for petroleum exploration: 1. A sea-floor equipment system, *Geophysics*, 63, 816–825.
- Edwards, R. N. (1997), On the resource evaluation of marine gas hydrate deposits using sea-floor transient electric dipole-dipole methods, *Geophysics*, 62, 63–74.
- Eidesmo, T., S. Ellingsrud, L. M. MacGregor, S. Constable, M. C. Sinha, S. Johansen, F. N. Kong, and H. Wester Dahl (2002), Sea bed logging (SBL), a new method for remote and direct identification of hydrocarbon filled layers in deepwater areas, *First Break*, 20, 144–152.
- Flosadóttir, A. H., and S. Constable (1996), Marine controlled-source electromagnetic sounding: 1. Modeling and experimental design, *J. Geophys. Res.*, 101, 5507–5517.
- Kvenvolden, K. (2000), Gas hydrate and humans, *Ann. N. Y. Acad. Sci.*, 912, 17–22.
- Kvenvolden, K. (2003), *Coastal Systems and Continental Margins Natural Gas Hydrate in Oceanic and Permafrost Environments*, vol. 5, *Natural Gas Hydrate: Background and History of Discovery*, edited by M. D. Max, pp. 9–16, Springer, New York.
- Schwalenberg, K., E. Willoughby, R. Mir, and R. N. Edwards (2005), Marine gas hydrate electromagnetic signatures in Cascadia and their correlation with seismic blank zones, *First Break*, 23, 57–63.
- Shipboard Scientific Party (2002), Leg 204 Preliminary Report, *Prelim. Rep. 104*, Ocean Drill. Program, Texas A&M Univ., College Station, Tex.
- Shipboard Scientific Party (2003), Leg 204 summary, in *Proceedings ODP, Initial Reports*, vol. 204, edited by A. M. Tréhu *et al.*, pp. 1–75, Ocean Drill. Program, Texas A&M Univ., College Station, Tex.
- Shibley, T. H., M. H. Houston, R. T. Buffler, F. J. Shaub, K. J. McMillen, J. W. Ladd, and J. Worzel (1979), Seismic evidence for widespread possible gas hydrate horizons on continental slopes and rises, *AAPG Bull.*, 63, 2204–2213.
- Sloan, E. D. (1990), *Clathrate Hydrates of Natural Gas*, Marcel Dekker Inc., New York.
- Torres, M. E., K. Wallmann, A. M. Tréhu, G. Bohrmann, W. Borowski, and H. Tomaru (2004), Gas hydrates growth, methane transport, and chloride enrichment at the southern summit of Hydrate Ridge, Cascadia margin off Oregon, *Earth Planet. Sci. Lett.*, 226, 225–241.
- Tréhu, A. M., and N. Bangs (2001), 3-D seismic imaging of an active margin hydrate system, Oregon continental margin report of cruise, *Rep. TTN112 182*, Oregon State Univ., Corvallis.
- Tréhu, A. M., G. Bohrmann, F. Rack, M. Torres, and Shipboard Scientific Party (2003), *Proceedings ODP, Initial Reports* [CD-ROM], vol. 204, edited by A. M. Tréhu *et al.*, Ocean Drill. Program, Texas A&M Univ., College Station, Tex.
- Tréhu, A. M., *et al.* (2004), Three-dimensional distribution of gas hydrate beneath southern Hydrate Ridge: Constraints from ODP Leg 204, *Earth Planet. Sci. Lett.*, 222, 845–862.
- Yuan, J., and R. N. Edwards (2000), The assessment of marine gas hydrates through electronic remote sounding: Hydrate without a BSR?, *Geophys. Res. Lett.*, 27, 2397–2400.
- Zhang, Z., and G. A. McMechan (2003), Elastic inversion and interpretation of seismic data from Hydrate Ridge, offshore Oregon, with emphasis on structural controls of the distribution and concentration of gas hydrate and free gas, Master's thesis, Cent. for Lithospher. Stud., Univ. of Tex. at Dallas, Richardson.

J. P. Behrens, S. C. Constable, K. W. Key, and K. A. Weitemeyer, Scripps Institution of Oceanography, La Jolla, CA 92093-0225, USA. (kweiteme@ucsd.edu)